Effect of Airfoil Geometry on Performance with Simulated Intercycle Ice Accretions

Andy P. Broeren[*] and Michael B. Bragg[†]

University of Illinois at Urbana-Champaign, Urbana, Illinois 61801

This paper presents the results of an experimental study designed to evaluate the performance effects of intercycle ice accretions on airfoils with different geometries. The intercycle ice accretions were simulated using combinations of various size grit roughness. These simulations were tested on three airfoils: NACA 23012, NACA 3415, and NLF 0414 at a Reynolds number of 1.8×10^6 and a Mach number of 0.18. Results from the NACA 23012 airfoil tests closely matched those from a previous study, validating the ice-shape simulation method. This also showed that a simple geometric (chord-based) scaling of the ice was appropriate. The simulated ice effect, in terms of maximum lift performance, was most severe for the NACA 23012 airfoil. The maximum lift coefficients were in the range of 0.65 to 0.80 for the iced configuration compared to a clean value of 1.47 for the NACA 23012 airfoil at this Reynolds number. In contrast, the maximum lift coefficients for the NLF 0414 airfoil with the same ice simulations were in the range of 0.90 to 1.05, compared to a clean value of 1.34. The results for the NACA 3415 with the simulated intercycle ice shapes were between the other two airfoils.

Nomenclature

C_d = drag coefficient
C_l = lift coefficient
$C_{l,\max}$ = maximum lift coefficient, coincident with α_{stall}
C_m = quarter-chord pitching-moment coefficient
C_p = pressure coefficient
c = airfoil chord length
k = roughness height or thickness
M = freestream Mach number
Re = freestream Reynolds number, based on chord
x = chordwise position along airfoil
y = normal position from airfoil chord line
α = airfoil angle of attack
α_{stall} = stalling angle of attack, coincident with $C_{l,\max}$

Introduction

THE cyclic operation of typical pneumatic aircraft deicing systems leads to the formation of residual and intercycle ice accretions. For example, pneumatic boots are usually activated every minute or every three minutes, depending upon the severity of icing. The ice accretion present on the deicer surface just prior to its initial activation is the preactivation ice. After the system has been cycled a sufficient number of times, the periodic activation and ice accretion cycle reaches steady state. After steady state has been reached, "intercycle" ice refers to the ice shape as it exists immediately before subsequent activations of the deicer. This is not to be confused with "residual" ice, which refers to any ice that remains on the surface immediately after the deicer operation. This paper addresses the aerodynamic performance penalties associated with intercycle ice accretions for three different airfoil geometries.

The characteristics of residual and intercycle ice accretions have been the subject of several previous investigations. Shin and Bond[1]

analyzed the ice accretions for several different deicing systems installed on a NACA 0012 airfoil model. They concluded that the intercycle ice would have an effect on airfoil and wing performance and that uniformly distributed roughness might not be an appropriate simulation of the actual intercycle ice. No aerodynamic measurements were performed during the study. Albright et al.[2] measured the variation in drag coefficient before and after the operation of a pneumatic deicer on a NACA 65_1-215 airfoil. Bowden[3] also showed how the lift coefficient for a NACA 0011 airfoil decreased as ice was accreted between deicer operations and then how the lift increased when the boot was operated and the ice shed. Although these results provided important insight into the performance effects of residual and intercycle ice accretions, the data were acquired at fixed angle of attack. Therefore, the airfoil stall characteristics with these ice accretions were not documented. Jackson and Bragg[4] and Gile-Laflin and Papadakis[5] investigated the effect of intercycle ice accretions on the stalling characteristics of an NLF 0414 airfoil. The performance degradation in maximum lift was on the order of 30% for both studies.

A more recent investigation using high-fidelity simulations of intercycle ice accretions showed significant airfoil performance degradations. Broeren et al.[6,7] generated intercycle ice accretions on a 3-ft chord NACA 23012 airfoil model equipped with pneumatic deicing boots. Molds were made of selected intercycle ice accretions that were later used to produce castings that were attached to the leading edge of a 3-ft chord NACA 23012 airfoil model used for aerodynamic testing. The aerodynamic testing was performed in a pressure tunnel where the Reynolds number was varied from 2.0×10^6 to 10.5×10^6 and the Mach number was varied from 0.10 to 0.28. Typical results showed that the intercycle ice accretions resulted in a 60% decrease in maximum lift. The authors suggested that this large performance penalty was related to the ridge-like features of the intercycle accretions and the sensitivity of the NACA 23012 airfoil to this type of ice shape. The 60% decrease was twice as large as the penalty for the NLF 0414 airfoil.[4,5]

Studies by Lee[8] and Lee and Bragg[9−11] have shown that the clean airfoil geometry (i.e., pressure distribution) can influence the aerodynamic severity of a spanwise-ridge ice accretion. These studies were carried out using a forward-facing quarter-round shape with normalized height k/c of 0.0139. The quarter-round was uniform in size and shape across the model span and was positioned at several different chordwise locations. Two of the airfoils tested with this simulated ice ridge were the NACA 23012m (a slightly modified version of the standard NACA 23012) and the NLF 0414. Some key results are summarized in Ref. 10. The lowest $C_{l,\max}$ on the NACA 23012 airfoil was 0.25 with the quarter-round located near

*Research Scientist, Department of Aerospace Engineering, 306 Talbot Laboratory, 104 S. Wright Street; broeren@uiuc.edu. Senior Member AIAA.

†Professor and Head, Department of Aerospace Engineering, 306 Talbot Laboratory, 104 S. Wright Street; mbragg@uiuc.edu. Associate Fellow AIAA.

$x/c = 0.12$. In contrast, the lowest $C_{l,\max}$ on the NLF 0414 was 0.68, and this did not vary significantly with ice-shape location between $x/c = 0.02$ and 0.20. The reason given for this difference was that the large leading-edge suction pressures on the clean NACA 23012 airfoil were prevented from forming in the iced case, thus resulting in the large lift reductions. The clean NLF 0414 had a relatively uniform chordwise pressure loading, and this was not as significantly affected by the ice shape, thus resulting in the smaller lift reductions.

The purpose of this paper is to demonstrate how the performance of three different airfoils was affected by the same intercycle ice-accretion simulation. The airfoils considered were the NACA 23012, NACA 3415, and the NLF 0414. These have pressure distributions and geometries that are significantly different. The intercycle ice shapes used in this investigation were adapted from those presented in Ref. 6. The ice-shape simulations were built up on the airfoil models using various sizes of grit roughness. Performance data were then acquired over a large angle-of-attack range, up to and including stall, at a Reynolds number of 1.8×10^6 and a Mach number of 0.18.

Experimental Methods

All of the aerodynamic testing was carried out at the University of Illinois Subsonic Aerodynamics Laboratory using the low-speed, low-turbulence wind tunnel. This wind tunnel is of open-return type with a 3×4-ft rectangular working section and a maximum speed of approximately 235 ft/s. The airfoil models all had a 1.5-ft chord and spanned the 3-ft height of the test section. The NACA 23012 airfoil was a single-element model, whereas the NACA 3415 and NLF 0414 airfoils each had a 25% chord simple flap. The airfoil models were supported by a three-component force balance located below the test section. The flap position was controlled by a two-member linkage system driven by a linear traverse. The traverse was mounted to the metric force plate of the balance. For the present series of tests, the flap angle was fixed at 0 degs, and the flap gap was sealed on the lower surface. All of the models had a dense distribution of pressure taps located in a main chordwise row near the midspan location and a secondary spanwise row. A traversable rake was used to obtain the airfoil wake-pressure profile. Both the wake pressures and model surface pressures were measured with an electronically scanned pressure system. More details about this experimental arrangement can be found in Lee.[8]

The lift coefficient C_l and pitching-moment coefficient C_m taken about the quarter-chord were derived from both the force balance and the surface-pressure measurements. The agreement in the results from these two methods was very good. In this paper only the values from the pressure measurements are shown for simplicity. The drag coefficient C_d was calculated from the wake pressures using standard momentum-deficit methods. All of these aerodynamic coefficients and the angle of attack were corrected for wall interference effects using the methods of Rae and Pope.[12] The experimental uncertainty in these coefficients was also estimated using the methods of Kline and McClintock[13] and Coleman and Steele[14] for 20:1 odds. Table 1 lists these uncertainties for a set of pressure-derived coefficients, except for the angle of attack, which was obtained directly from the force balance system. The values were determined by Lee[8] and Lee and Bragg[11] for freesteam conditions of $Re = 1.8 \times 10^6$ and $M = 0.18$. The relative uncertainty in C_m seems large for this example owing to the small reference value. For cases where the C_m values were larger, the absolute uncertainty would be similar, therefore resulting in a lower relative uncertainty.

The intercycle ice-accretion simulations tested on the three airfoils were adapted from those recorded and presented in Refs. 6 and 15. In that work, four accretions were selected for testing in the NASA Langley Low-Turbulence Pressure Tunnel (LTPT). They were designated by the numbers 290, 296, 312 and 322, after the icing run number. The ice-shape castings used for the LTPT experiments in Refs. 6 and 15 represented the highest-fidelity simulation because the ice accretions had very irregular roughness sizes and spanwise variation. Despite this, a common characteristic among the ice shapes was spanwise ridge-like features that were distinct formations in the roughness. Both the ice accretion and aerodynamic tests were carried out using a 3-ft chord NACA 23012 airfoil. Therefore, the simulations were scaled down by a factor of two when simulated on the 1.5-ft chord models used in the present investigation. The relative chordwise locations of ice-shape features (such as characteristic ridges) were also preserved for these experiments. For example, an ice feature located at $x/c = 0.04$ would be maintained for each airfoil, even though the distance measured along the surface would be slightly different. The authors concede that the character of the ice accretions can be different if accreted on each of the three airfoils separately. However, this did not compromise the main objective of this study, which was to determine the effect of airfoil geometry on the performance degradation. In fact, to determine the effect of airfoil geometry on the aerodynamics with intercycle ice the same ice simulation must be tested on each airfoil.

The intercycle ice simulations for the present experiments were constructed from various sizes of loose grit roughness. This material was useful for representing the surface irregularities of the actual ice accretions. These roughnesses were applied to the models using a substrate of double-sided tape. The chordwise distribution of ice thickness was controlled by using roughness of different sizes. Ridge-like features were built up at the appropriate chordwise location by layering the roughness. A spray adhesive was used to hold the roughness in place. Spanwise variation was also incorporated into the simulations, but with less fidelity as compared to the chordwise variations. Figure 1 shows a comparison of an actual ice shape (on a 3-ft chord model) with the roughness simulation (on an 1.5-ft chord model). Figure 2 compares the tracings of the other three intercycle ice shapes. The bottom photograph in Fig. 1 also illustrates how the ice-shape simulation was placed on either side of the pressure tap row so that a reasonable representation of the pressure distribution around the ice-shape simulation could be measured. The lift and pitching moment determined from integration of the pressure distribution agreed very well with the force-balance data.

In addition to the intercycle ice simulations, the airfoil models were also tested with standard roughness in the form of 80- and 150-grit paper-backed garnet sandpaper. These tests were conducted because sandpaper roughness is often used by industry to represent residual and intercycle ice. Also, the sandpaper provides a very repeatable form of roughness that could be identically duplicated on each of the airfoil models. As shown in Table 2, these grit sizes approximately represented the chord length scaled equivalent of the 40- and 80-grit sizes that were tested at the LTPT.[6,15] The roughness heights listed in the table do not include the thickness of the paper backing that was approximately one and a half times as large as the roughness itself. Also, 0.003-in.-thick double-sided tape was used to attach the sandpaper to the model. The surface extent of the sandpaper roughness was $x/c = 0.10$ on the lower surface to $x/c = 0.07$ on the upper surface and was placed on either side of the pressure orifices, similar to Fig. 1.

Table 1   Estimated experimental uncertainties

Aerodynamic quantity	Reference value	Absolute uncertainty	Relative uncertainty, %
α	5.00 deg	±0.02 deg	±0.40
C_p	−0.712	±0.0037	±0.52
C_l	0.633	±0.00211	±0.33
C_m	−0.0089	±0.000349	±3.90
C_d	0.0102	±0.000143	±1.40

Table 2   Comparison of sandpaper roughness heights

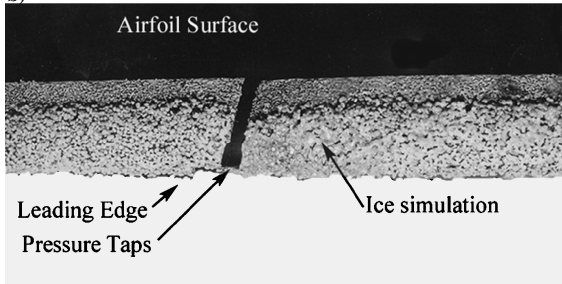| Sandpaper grit number	Roughness height[a] k, in.	Normalized height k/c for $c = 3$ ft	Normalized height k/c for $c = 1.5$ ft
40	0.0205	0.00057	0.00114
80	0.0083	0.00023	0.00046
150	0.0041	0.00011	0.00023

[a]Based on nominal size of commercial carborundum.[12]
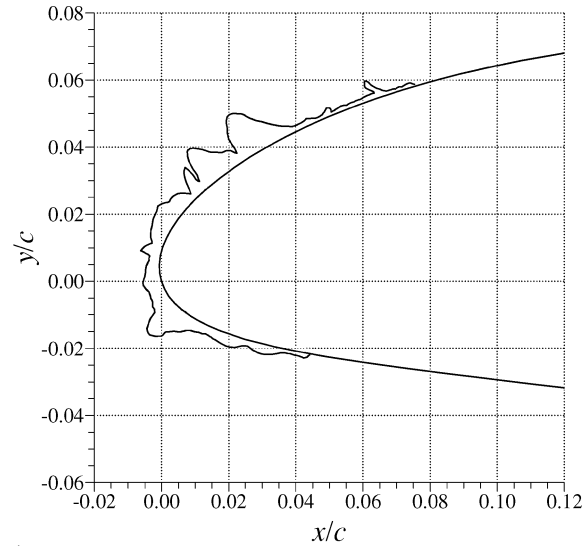
a)
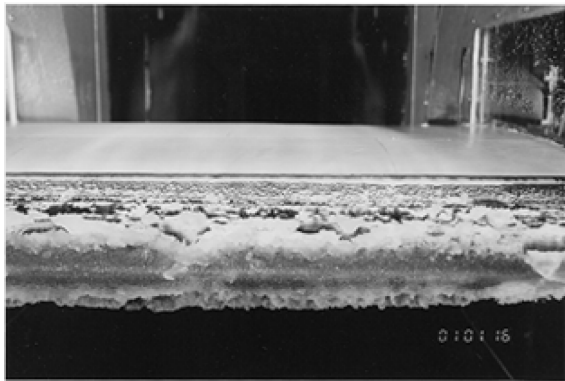
b)

c)

Fig. 1   Comparison between ice-shape 290 a) tracing and b) photograph with c) the roughness simulation.

Fig. 2   Comparison of three intercycle ice-shape tracings.

Results

Clean Airfoil Performance Comparisons

The three airfoils tested in this study were selected because their clean aerodynamic characteristics were substantially different. This is illustrated in the performance plot of Fig. 3 for data acquired at $Re = 1.8 \times 10^6$ and $M = 0.18$. The lift data show that the NACA 23012 airfoil had the highest $C_{l,\max}$ of about 1.47. This was followed by the NACA 3415 ($C_{l,\max} = 1.37$) and the NLF 0414 ($C_{l,\max} = 1.34$). The lift curve for the NLF 0414 airfoil exhibited a distinct change in slope near $\alpha = 2$ deg. This resulted from trailing-edge separation aft of about $x/c = 0.70$ on the airfoil upper surface. The pitching-moment data show that the NACA 23012 had the lowest values, followed by the NACA 3415 and then the NLF 0414 airfoil. This indicated that the NACA 23012 had the least amount of positive camber. The NLF 0414 had the lowest drag in the range of $-3 < \alpha < 3$ deg., because it was a laminar-flow airfoil. For angles of attack greater than 3 deg, there was significant flow separation at this Reynolds number aft of about $x/c = 0.70$ on the
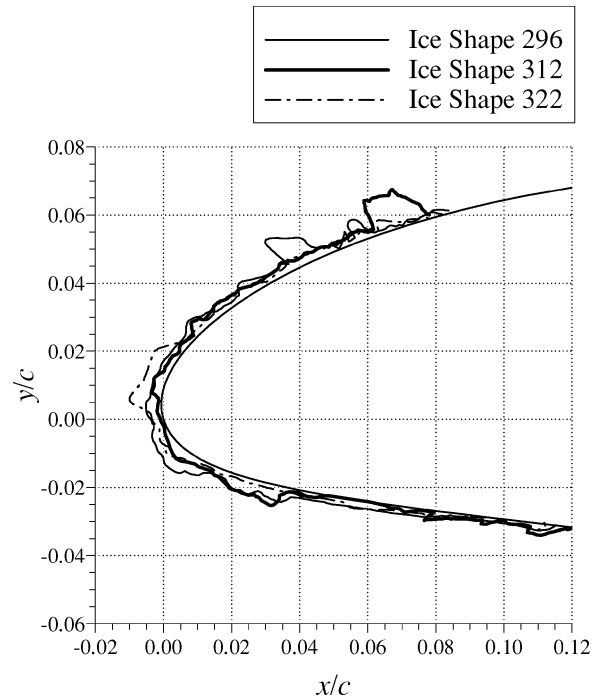
upper surface, which resulted in higher drag than the two NACA airfoils.

The differences in these airfoils are even more evident in the pressures distributions. An example is shown in Fig. 4 for a nominal lift coefficient of 0.6. This corresponded to different angles of attack for each airfoil as indicated by Fig. 3. The pressure distributions for the NACA 3415 and NLF 0414 airfoils show the expected discontinuities near $x/c = 0.75$ as a result of the flap gap. The NACA 23012 airfoil had a very large suction peak (with $C_{p,\min} = -1.6$) centered near $x/c = 0.06$. There was a severe pressure recovery (with very large adverse pressure gradient) from $x/c = 0.08$ to 0.22. The pressure recovery was more gradual downstream of this location and extended to the trailing edge. The NACA 3415 airfoil had a pressure distribution that was quite different. A large suction peak was not present on this airfoil at this angle of attack; however, a $C_{p,\min}$ value of -1.2 was located near $x/c = 0.18$. Thus the pressure recovery here was more gradual. The pressure gradient was nearly constant from $x/c = 0.25$ to the trailing edge. The NLF 0414 airfoil had a nearly constant suction pressure between $x/c = 0.04$ to 0.72. Downstream of this location, there was a very severe adverse gradient that led to the trailing-edge flow separation just described.

Validation of Ice Simulation Method

The method of simulating the intercycle ice accretions on the 1.5-ft chord model was validated by comparing results with the previous LTPT tests of the intercycle ice castings. Comparisons were first conducted for the clean airfoil baseline to ensure that differences in iced-airfoil performance between the two facilities could be attributed to the ice simulation method. The NACA 23012 airfoil was tested in the clean configuration at the LTPT (using the 3-ft chord model) and at the University of Illinois (using the 1.5-ft chord model) for the present tests. These results are plotted in Fig. 5 for closely matched Reynolds- and Mach-number conditions. The data show good agreement in the lift curve until the maximum lift region, where the LTPT data had a slightly higher $C_{l,\max}$ value. This discrepancy is small and might even have been attributable to the small difference in Reynolds number or model installation effects. At the LTPT, each end of the airfoil model was sealed against the side walls, and a suction system was employed. Broeren et al.[6,7] and Broeren and Bragg[15] provide more details about the model installation and side-wall suction system. At Illinois, there were small gaps between each end of the airfoil model and the side walls.
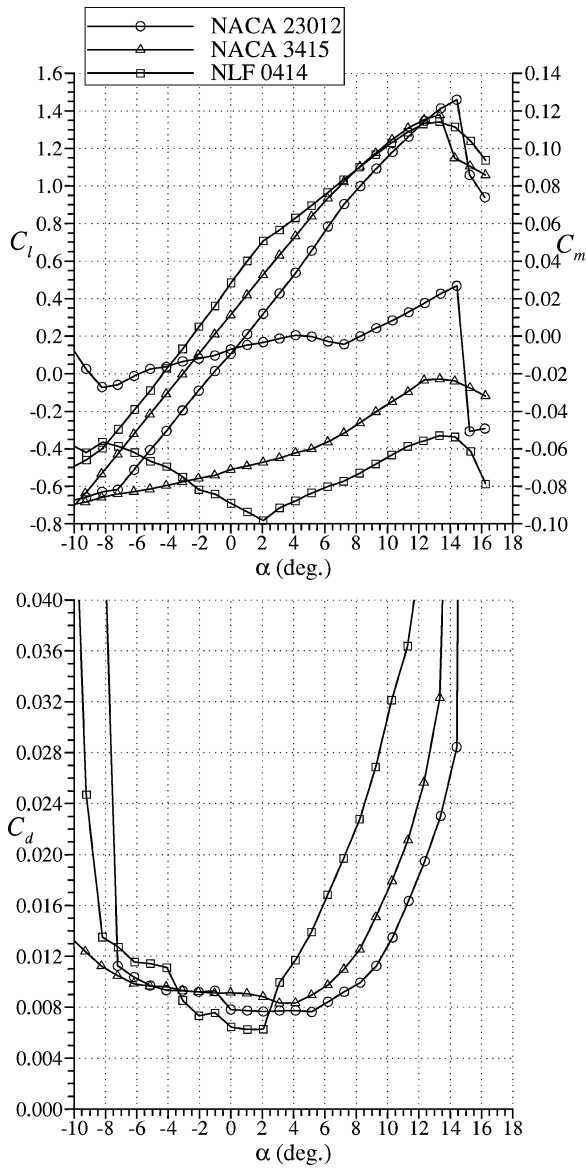
Fig. 3   Comparison of the clean airfoil performance at $Re = 1.8 \times 10^6$ and $M = 0.18$.
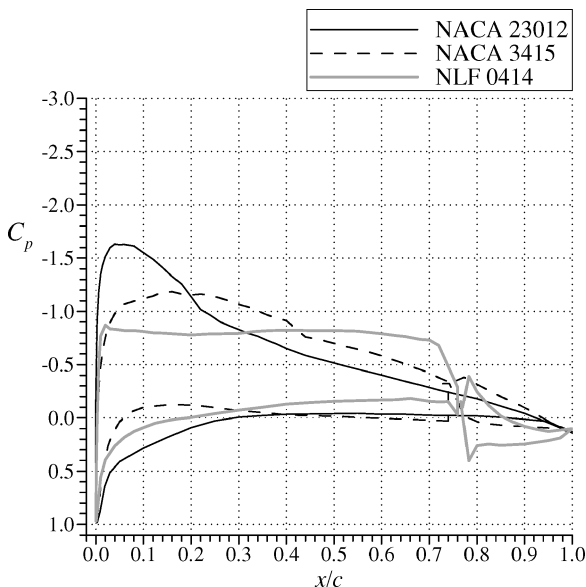

Fig. 4   Comparison of clean airfoil pressure distributions at approximately matched $C_l = 0.6$.
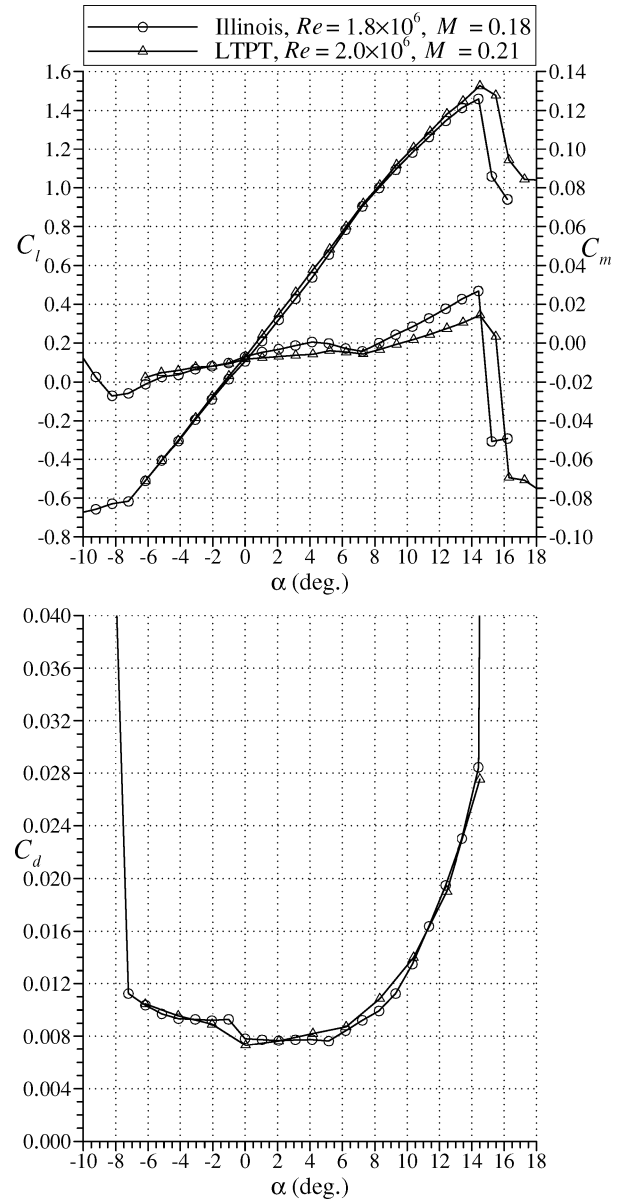

Fig. 5   Comparison of the Illinois NACA 23012 airfoil performance data with LTPT results from Broeren et al.[6,7]

The effect of these gaps on $C_{l,max}$ was believed to be small based upon comparison of the force balance and integrated pressure data as well as comparisons to existing data for other airfoils. The Illinois pitching-moment data were slightly more nonlinear. Agreement in the drag values is good except at certain odd angles of attack (e.g., −1 and 5 deg). Comparison here is difficult because there were no wake-survey drag data available in the LTPT data set for odd numbered angles of attack. Despite these minor discrepancies, the cross-facility comparison is good.

The intercycle ice castings tested at the LTPT were considered the highest-fidelity representation of the ice accretions that could be used for aerodynamic testing. Detailed comparisons with the half-scale roughness simulation results are plotted for two of the four ice shapes in Fig. 6. The lift data show that the half-scale simulations were very effective in reproducing the lift-performance degradations. In the iced-airfoil case, model installation effects should be smaller than for clean airfoils owing to the lower maximum lift coefficients and modified stall mechanisms resulting from the ice shapes. Agreement in the pitching-moment data was not as good, but the general trends were certainly represented in the Illinois data. The agreement in the drag values was reasonable. Similar comparisons were observed for the other two ice shapes. These data indicate that
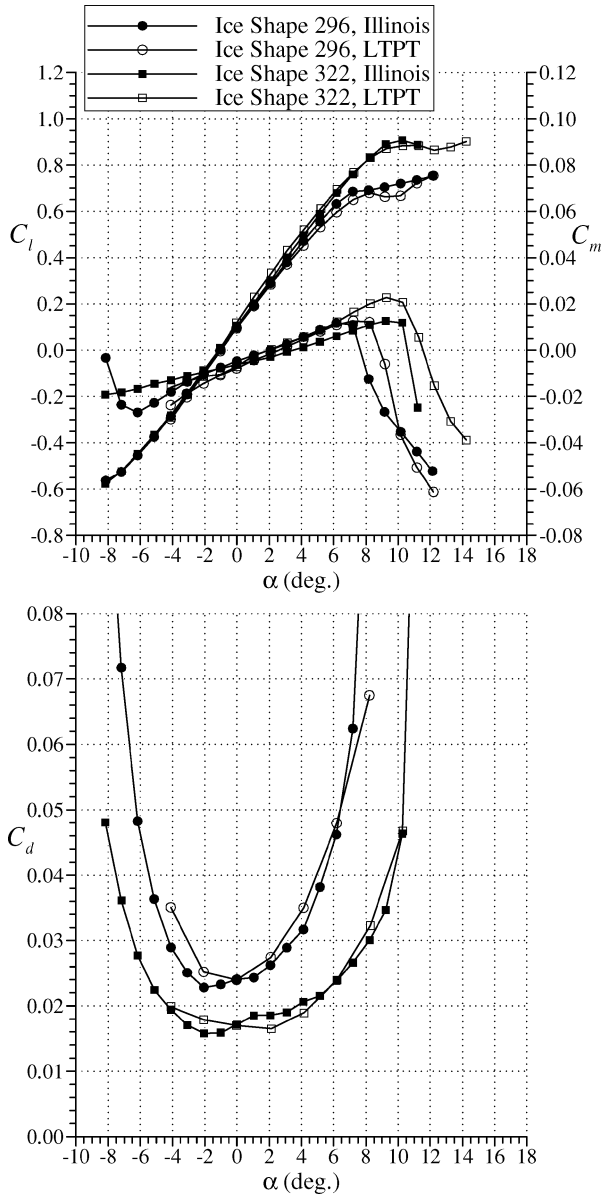
Fig. 6 Comparison of Illinois and LTPT performance data for the NACA 23012 with simulated intercycle ice shapes. Illinois data at $Re = 1.8 \times 10^6$ and $M = 0.18$ and LTPT data at $Re = 2.0 \times 10^6$ and $M = 0.10$ after Broeren et al.[6,7]

Fig. 7 Comparison of Illinois and LTPT performance data for the NACA 23012 with sandpaper roughness. Illinois data at $Re = 1.8 \times 10^6$ and $M = 0.18$ and LTPT data at $Re = 2.0 \times 10^6$ and $M = 0.10$ after Broeren et al.[6,7]

the methods used to simulate the intercycle shapes on the 1.5-ft chord models were valid, at a minimum for these particular ice shapes on the NACA 23012 airfoil. The data also show that a simple geometric scaling is appropriate for ice features of this type and size.

In addition to the intercycle ice-shape simulation tests, standard roughness was also applied to the airfoil leading edge. For tests on the 3-ft chord LTPT model, 40- and 80-grit sandpaper was used. The geometrically scaled equivalent sized sandpaper for the 1.5-ft chord model used for the present tests was nominally 80- and 150-grit (compare Table 2). An example of this comparison is given in Fig. 7 for the 40-/80-grit case. The maximum lift values from both tests were nearly identical, whereas the stalling angle of attack was 1 deg lower for the Illinois data. This angle-of-attack discrepancy is small and could be less than 1 deg if the data were acquired in smaller increments. Agreement in the pitching-moment variation with angle of attack was not quite as good between the two tests. Similarly, agreement in the measured drag values was very good, except over the range of $-2 < \alpha < 4$ deg. Despite these small discrepancies, the data show that the geometric scaling of the roughness height was also appropriate for this case. Analogous results were obtained for the 80-/150-grit comparison.
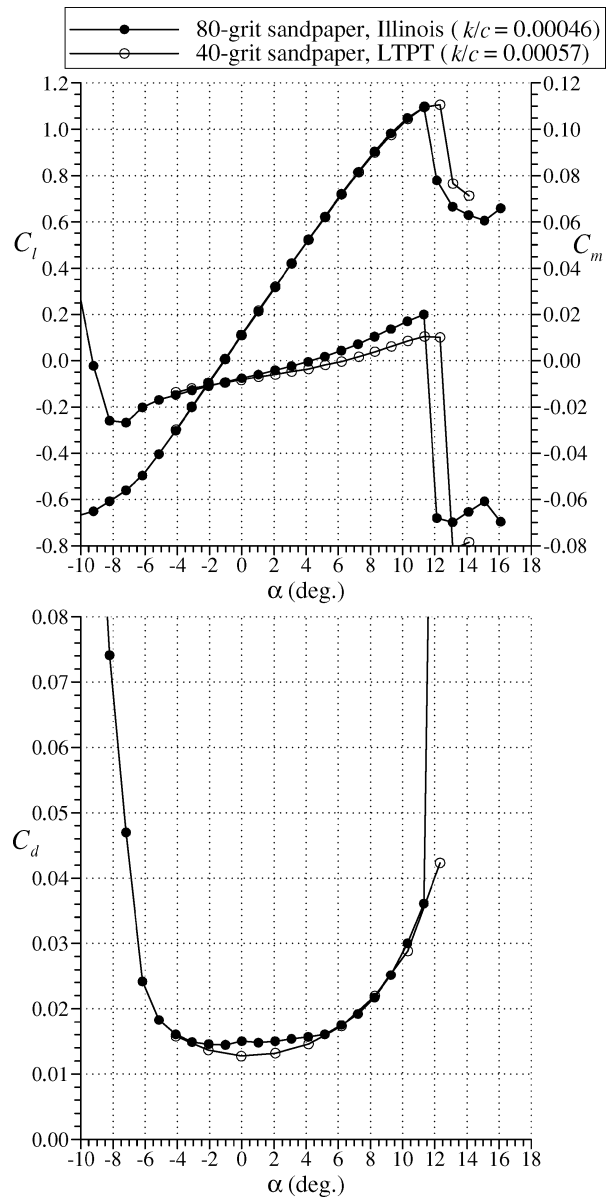
Iced-Airfoil Performance Comparisons

The effect of the intercycle ice shapes on the performance of the NACA 23012 airfoil was thoroughly discussed in Broeren et al.[6,7] The data shown in Fig. 8 were acquired at Illinois using an 1.5-ft chord airfoil model and the built-up roughness simulations of the intercycle ice accretions. As noted in the previous studies, the intercycle ice had a very significant effect on airfoil performance, especially in terms of maximum lift degradation. Three of the four intercycle shapes caused $C_{l,max}$ values in the range of 0.65 to 0.80 and stall angles in the range of 7 to 10 deg. The remaining ice shape 322 had a slightly higher $C_{l,max}$ value of about 0.90. An iced-airfoil $C_{l,max}$ value of 0.70 amounted to a 52% reduction from the clean value of 1.47. The intercycle shapes produced a stronger angle-of-attack dependence in the pitching moment at higher angles of attack. The minimum drag values increased by a factor of two to three from the clean case.

The performance effects of the 80- and 150-grit sandpaper roughness are summarized in Fig. 9 for the NACA 23012 airfoil at $Re = 1.8 \times 10^6$ and $M = 0.18$. The data show that the lift degradation caused by the uniform roughness was very significant with
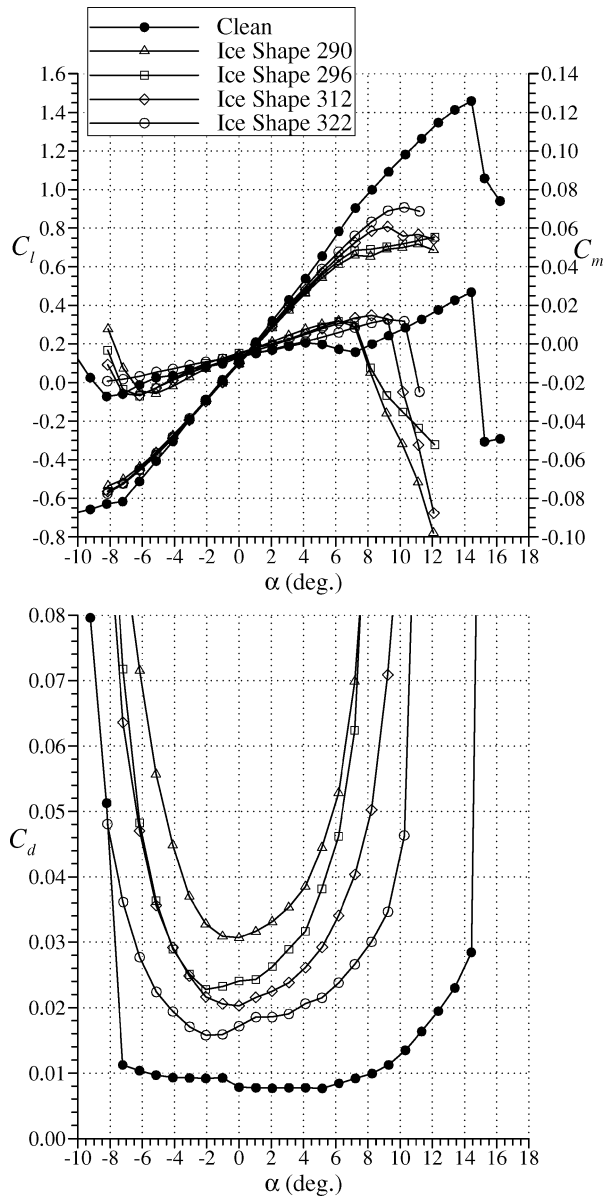
Fig. 8 Effect of intercycle ice simulations on NACA 23012 airfoil performance at $Re = 1.8 \times 10^6$ and $M = 0.18$.

Fig. 9 Effect of 80- and 150-grit sandpaper roughness on NACA 23012 airfoil performance at $Re = 1.8 \times 10^6$ and $M = 0.18$.

$C_{l,max}$ values near 1.10. However, these were substantially higher maximum lift values than for the airfoil with the intercycle ice simulations. Also noteworthy is the fact that there was very little difference in the lift performance between the 80- and 150-grit sandpaper, despite the almost two-fold difference in roughness height (compare Table 2). The effect of the uniform roughness on the pitching moment was similar to that caused by the ice-shape simulations. The drag values were increased from the clean case by less than a factor of two in the linear range of the lift curve. Broeren et al.[6,7] explain that the difference between the sandpaper roughness and intercycle ice results are reasonable because the former had a very uniform array of roughness, whereas the latter contained ridge-like features that were far from uniform. Another factor was that even the larger uniform roughness (80 grit) was considerably smaller in size than the actual accretions. For example, the nominal height (ignoring the larger ridge-like features) of ice shape 296 was on the order of $k/c = 0.0050$ (compare Fig. 1). This was more than a factor of 10 larger than the height of the 80-grit sandpaper at $k/c = 0.00046$ (compare Table 2). These results tend to support the conclusions of Shin and Bond[1] that uniform roughness might not be an adequate method for simulating intercycle ice.

The intercycle ice-shape simulations were tested on the NLF 0414 and NACA 3415 airfoils to gauge their sensitivity to this type of ice
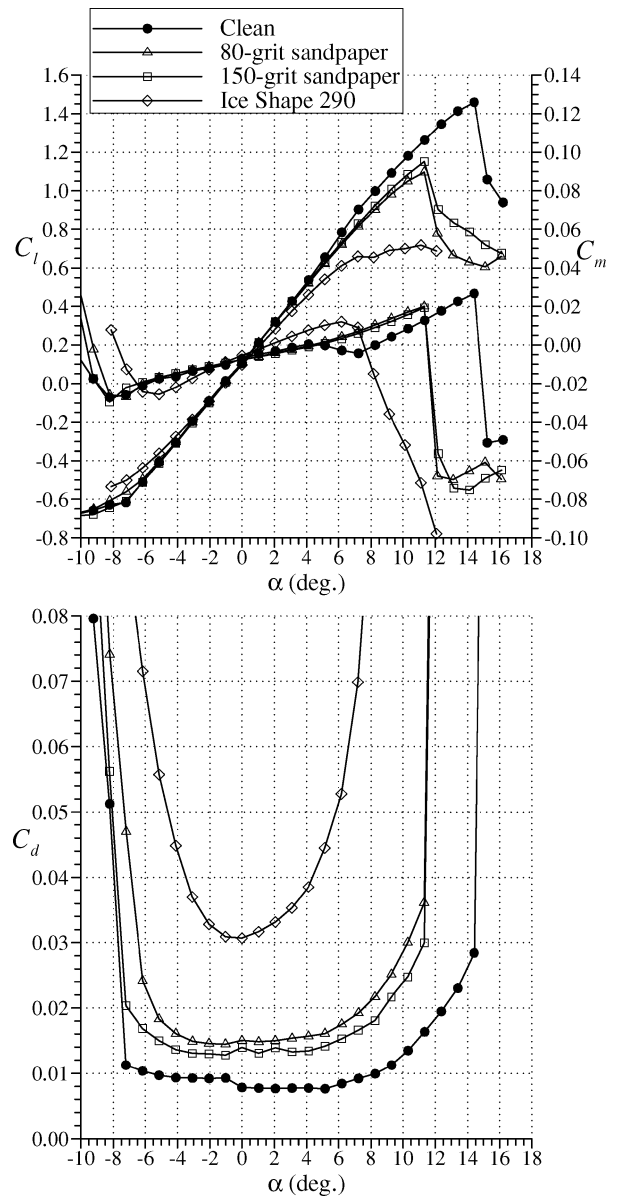
shape. Significant degradations in performance were also observed. The results for the NLF 0414 airfoil are shown in Fig. 10. The stall behavior with the ice simulations was similar to the NACA 23012 data in that there was a large range of $C_{l,max}$ from 0.90 to 1.05. The same ice shape 322 also resulted in the highest $C_{l,max}$. These iced-airfoil lift coefficients were significantly higher than the range for the ice simulations on the NACA 23012 airfoil which was 0.65 to 0.90. For example, an iced airfoil $C_{l,max}$ value of 0.95 constituted a 29% reduction from the clean value of 1.34. This is consistent with that reported by Jackson and Bragg[4] for other intercycle ice simulations tested on the NLF 0414 airfoil. This value is slightly more than half of the 52% reduction in maximum lift observed for the NACA 23012 airfoil.

A key difference in lift performance with the ice simulations between the two airfoils was observed for lift coefficients in the range of 0.0 to 0.6. In this range, the simulated ice had a more severe effect on the NLF 0414 airfoil than on the NACA 23012, as there were larger differences between the clean and iced lift coefficients. That is, the intercycle ice simulations resulted in a lower lift-curve slope for the NLF 0414 airfoil than for the NACA 23012 airfoil. The effect of the simulated ice on the NLF 0414 airfoil pitching moment and drag were also similar to the effects on the NACA 23012 airfoil performance.
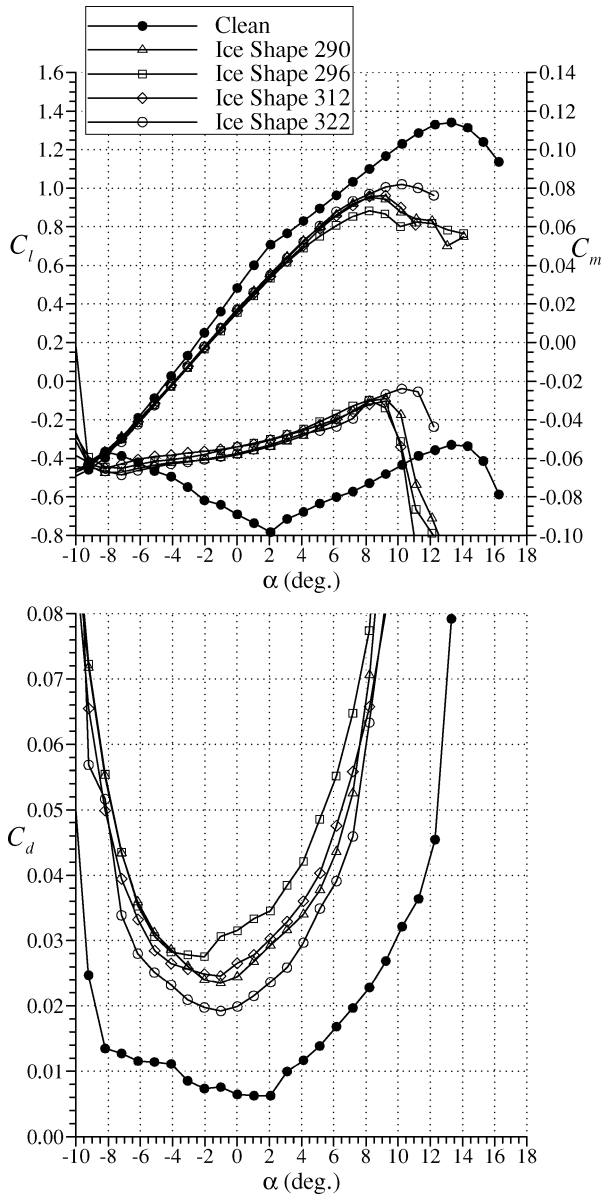
Fig. 10   Effect of intercycle ice simulations on NLF 0414 airfoil performance at $Re = 1.8 \times 10^6$ and $M = 0.18$.

Fig. 11   Effect of intercycle ice simulations on NACA 3415 airfoil performance at $Re = 1.8 \times 10^6$ and $M = 0.18$.

The performance of the NACA 3415 airfoil with the intercycle ice simulations was similar to the NLF 0414 airfoil as depicted in Fig. 11. In this case, there was less variation in maximum lift coefficient with the different ice shapes. The $C_{l,\max}$ values ranged from about 0.85 to 0.95. An iced-airfoil $C_{l,\max}$ of 0.90 constituted a 34% reduction from the clean value of 1.37. This reduction is more similar to the NLF 0414 airfoil performance than for the NACA 23012 with the same simulated ice shapes. The lift penalties (reduction in lift-curve slope) caused by the ice shapes for the NACA 3415 airfoil were very similar to the NLF 0414 airfoil in the range of $C_l = 0.0$ to 0.6. The effects on pitching moment and drag were also similar to the other airfoils.

The NLF 0414 and NACA 3415 airfoils were also tested with the uniform roughness applied to the leading edge of the airfoils. Results for the NLF 0414 airfoil are shown in Fig. 12. As with the intercycle ice simulations, the sandpaper roughness caused significantly smaller reductions in maximum lift from the clean value for this airfoil as compared to the NACA 23012 airfoil. However, the roughness altered the stalling characteristics such that there was a significant drop in lift beyond $C_{l,\max}$. This change in stall behavior from the clean case with the roughness present was not observed for the other two airfoils.
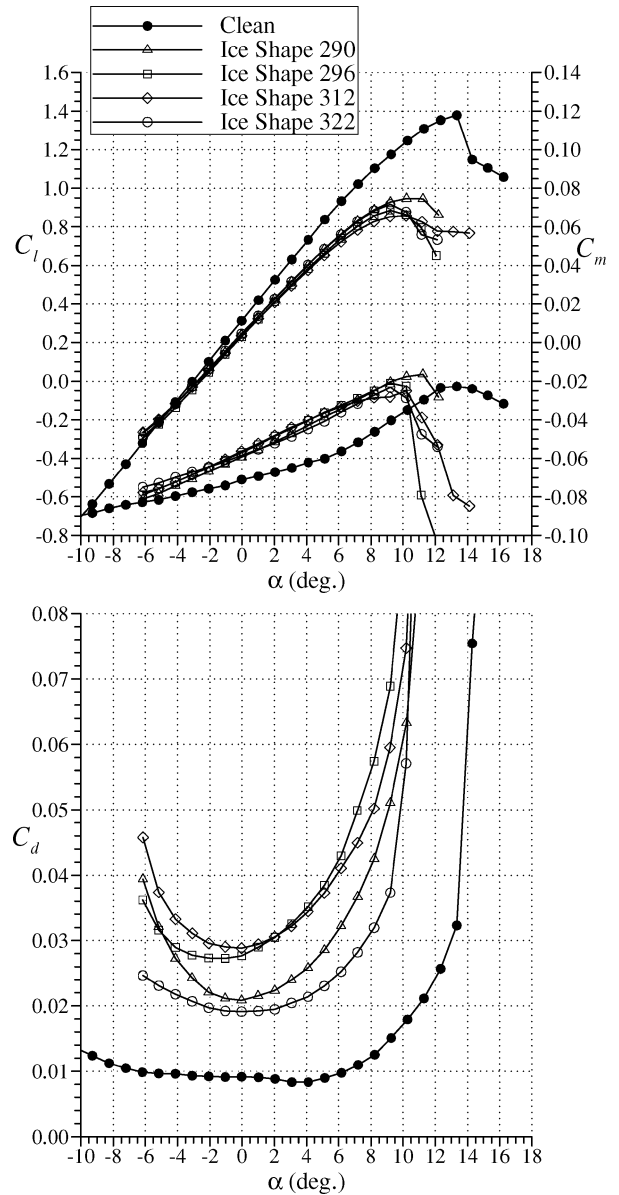
Discussion

Airfoil and Ice-Shape Geometry Effects

The effect of the intercycle ice simulations on maximum lift is summarized in Fig. 13 for the three airfoils tested. The chart re-iterates the preceding results that these ice shapes had the most severe effect, in terms of maximum lift degradation, for the NACA 23012 airfoil. On the other hand, the maximum lift values for the NLF 0414 airfoil were least affected by the intercycle ice shapes. The NACA 3415 airfoil results were similar to the NLF 0414 data for ice shapes 290 and 296. For the remaining two ice shapes, the NACA 3415 $C_{l,\max}$ values were between the NACA 23012 and NLF 0414 results. All four of the intercycle ice simulations tested were based on ice accretions at $\alpha = 0$ deg. Intercycle ice accretions generated at different angles of attack might have different characteristics that could affect the performance of each airfoil differently. Such parametric variation of ice features has been the subject of previous research (e.g., see Lee and Bragg[9]). The uniform roughness results were somewhat more mixed, given that the NACA 3415 airfoil had the lowest $C_{l,\max}$ values for each case. However, because the clean $C_{l,\max}$ value for the NACA 23012 airfoil was larger, the percentage degradation, at this Reynolds number, was larger for the NACA 23012.
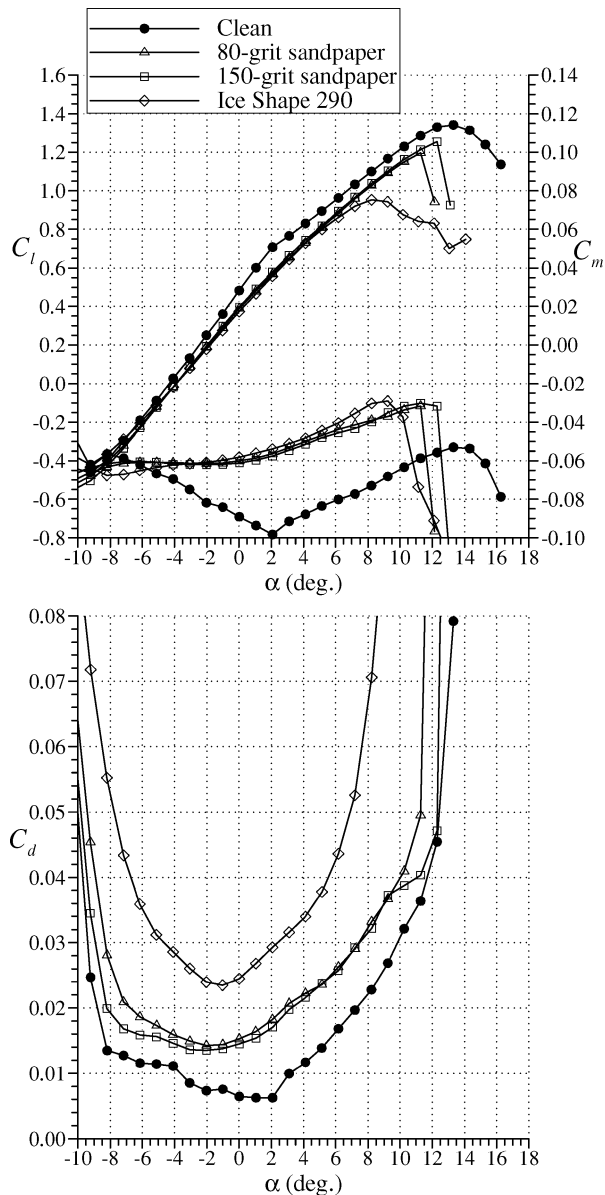
Fig. 12   Effect of 80- and 150-grit sandpaper roughness on NLF 0414 airfoil performance at $Re = 1.8 \times 10^6$ and $M = 0.18$.
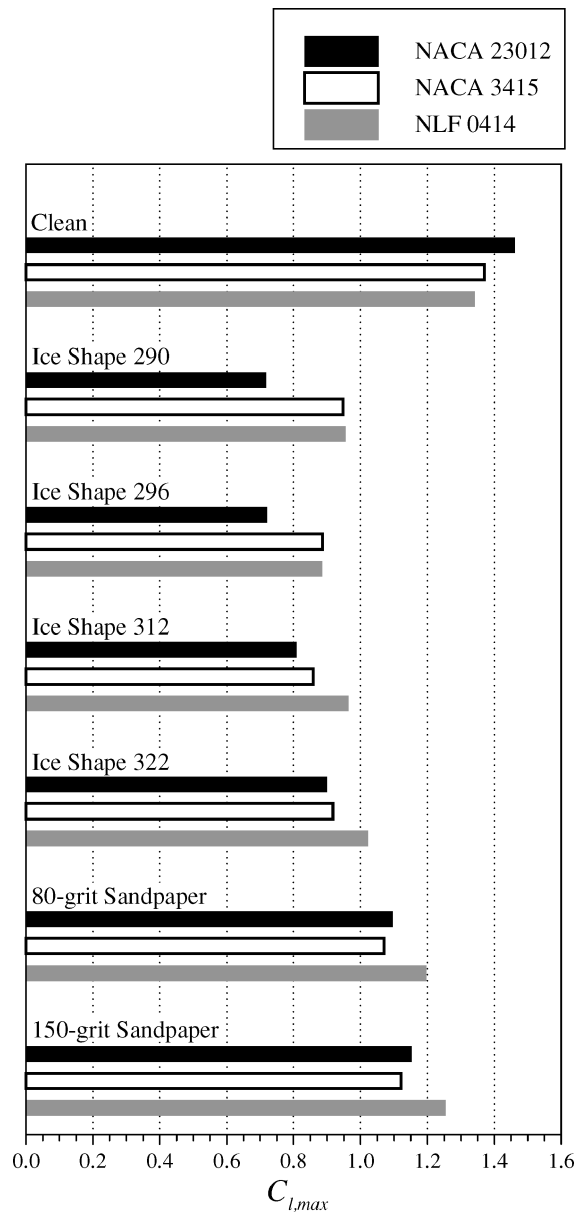

Fig. 13   Summary of intercycle ice simulations and sandpaper roughness effect on maximum lift for the three airfoils tested at $Re = 1.8 \times 10^6$ and $M = 0.18$.

If a chart similar to Fig. 13 were created for lift penalties in the range of clean $C_l = 0.0$ to 0.6, it would show that the intercycle ice simulations resulted in more severe lift penalties for the NACA 3415 and NLF 0414 airfoils. This effect is illustrated in Figs. 14 and 15. The pressure distributions are plotted for the NACA 23012 and the NLF 0414 airfoils at a clean $C_l \approx 0.5$ and with the ice-shape 296 simulation at the same angle of attack. For the NACA 23012 airfoil (Fig. 14), the ice simulation did not significantly alter the clean pressure distribution. The iced-airfoil lift coefficient of 0.47 was reduced about 13% from the clean value of 0.54. There was a higher suction peak owing to the local flow acceleration around the ice roughness. This was followed by a more severe adverse pressure gradient up to $x/c \approx 0.25$, where the clean and iced pressure distributions were very similar. There was some small divergence of the trailing-edge pressure that was perhaps indicative of boundary-layer separation. In the case of the NLF 0414 airfoil (Fig. 15), small suction peaks caused by the ice shape were evident on both the upper and lower surfaces. This resulted in significantly lower suction pressures on the upper surface from $x/c \approx 0.15$ to 0.75. In this case the iced-airfoil C_l was 0.35 compared to the clean value of 0.48 for the same angle of attack. This 27% reduction was about two times larger than for the NACA 23012 airfoil. Very similar results were observed for the NACA 3415 airfoil. Therefore, the lift of airfoils having a more

uniform pressure loading might have a greater sensitivity to this type of ice accretion than forward-loaded sections like the NACA 23012 over the range of low-to-moderate lift coefficients.

The large reductions in maximum lift caused by the intercycle ice accretions on the NACA 23012 were related to the pressure distribution on the clean airfoil. Lee[8] and Lee and Bragg[9-11] explored this airfoil-sensitivity concept in great detail and concluded that more forward-loaded airfoils (like the NACA 23012) were more sensitive to protuberances located over the first 20% chord. Broeren et al.[6,7] applied these findings to the intercycle ice shape results from the LTPT tests of the NACA 23012 airfoil. The NLF 0414 and NACA 3415 airfoil results of this study show that this airfoil-sensitivity concept can also be successfully applied to intercycle ice shapes on other airfoils. This is an important point because the quarter-round ice simulations of Lee[8] and Lee and Bragg[9-11] were not used to simulate a specific ice accretion. Instead, the quarter-round geometry was chosen to be representative of a class of ice accretion (super-cooled, large-droplet ice ridges downstream of ice-protected surfaces). In the present study, the intercycle ice-shape simulations represented specific ice accretions, and the performance results indicate that more forward-loaded airfoils tend to have larger reductions in maximum lift with ice accretion.
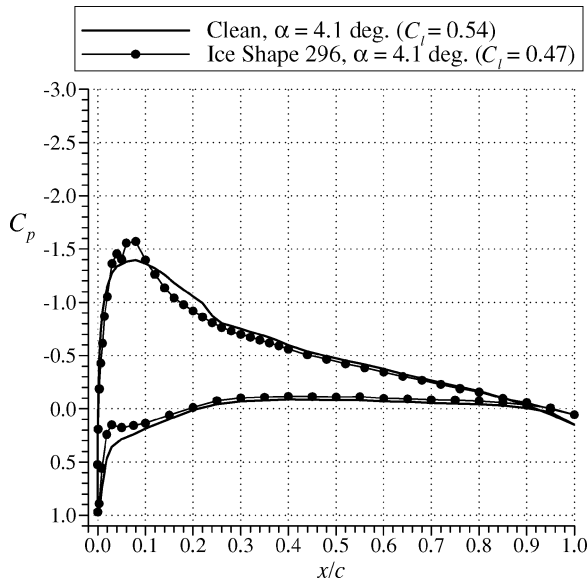
Fig. 14   Comparison of clean and iced pressure distributions for the NACA 23012 airfoil at matched angle of attack based on a clean $C_l \approx 0.5$.
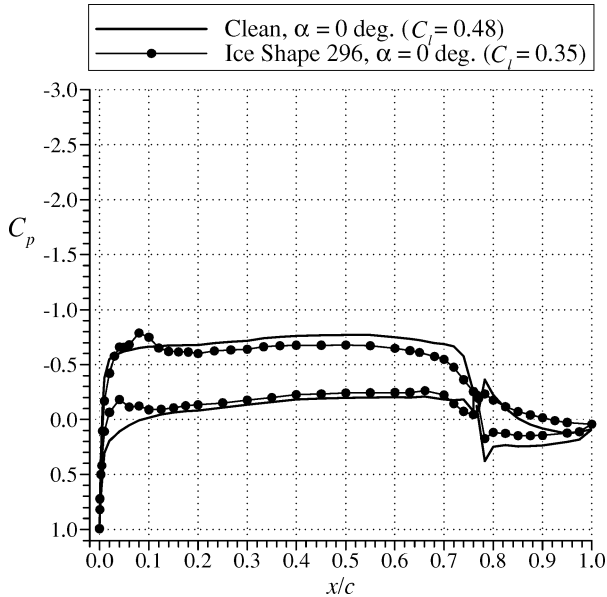

Fig. 15   Comparison of clean and iced pressure distributions for the NLF 0414 airfoil at matched angle of attack based upon a clean $C_l \approx 0.5$.

Comment on Reynolds-Number Effects

The data from the Illinois wind tunnel presented here were all acquired at $Re = 1.8 \times 10^6$ and $M = 0.18$. Broeren et al.[6,7] investigated the effects of Reynolds number and Mach number from $Re = 2.0 \times 10^6$ to 10.5×10^6 and $M = 0.10$ to 0.28. They found that there was only a small (less than 0.05) increase in maximum lift coefficient between $Re = 2.0 \times 10^6$ and 3.5×10^6 for the NACA 23012 airfoil with each of the four intercycle ice accretions. The 40- and 80-grit sandpaper cases had about 0.10 increase in $C_{l,\max}$. There was virtually no change in $C_{l,\max}$ for Reynolds numbers larger than 3.5×10^6. Similar results were reported by Addy and Chung[16] for tests of glaze-ice simulations on an NLF 0414 airfoil. Also, a large glaze-ice simulation was tested on a multi-element supercritical airfoil by Morgan et al.[17] Performance measurements were carried out on the model in the cruise configuration over a Reynolds number range of 3.0×10^6 to 12.0×10^6, and only very minor changes in maximum lift were observed for the iced-airfoil case. Therefore, the results of the present study should be applicable for higher Reynolds numbers. The caveat is that the clean maximum lift performance of

the airfoils considered in this study is Reynolds number dependent. For example, Broeren et al.[6,7] reported a clean $C_{l,\max}$ value of 1.80 for the NACA 23012 at $Re = 10.5 \times 10^6$ and $M = 0.21$. This is significantly higher than the value of 1.47 reported here for $Re = 1.8 \times 10^6$ and $M = 0.18$. Given that an intercycle iced-airfoil maximum lift coefficient of 0.70 would be relatively invariant over this Reynolds-number range, the performance penalty would be 61% at $Re = 10.5 \times 10^6$, instead of 52% at $Re = 1.8 \times 10^6$. However, clean maximum lift values for these and other airfoils are more readily obtainable from historical data and/or computational methods. For the NLF 0414 airfoil, Addy and Chung[16] give a clean $C_{l,\max}$ value of about 1.70 at $Re = 10.0 \times 10^6$ and $M = 0.21$. Using an iced $C_{l,\max}$ value of 0.95 yields a 44% reduction instead of the 29% reported here. Data for the NACA 3415 airfoil are more scarce, but an estimate can be made from Abbott and von Doenhoff,[18] who supply data for the NACA 2415 and NACA 4415 sections. These airfoils are "brothers" to the NACA 3415 and have nearly identical $C_{l,\max}$ values of 1.62 at $Re = 9.0 \times 10^6$ and $M \leq 0.17$. Therefore, a similar $C_{l,\max}$ value would be expected for the NACA 3415 airfoil. Using an iced maximum lift coefficient of 0.95 yields a 44% reduction instead of the 34% reported here. These examples show how the iced-airfoil data acquired at smaller scale and lower Reynolds number can be applied to higher Reynolds-number cases.

Summary

The purpose of this paper was to evaluate the sensitivity of airfoil geometry to the aerodynamic performance effects of intercycle ice accretions. Wind-tunnel tests with simulated intercycle ice shapes were conducted on the NACA 23012, NACA 3415, and NLF 0414 airfoils. These sections have geometries and pressure distributions that are substantially different. The intercycle ice shapes used in this study were adapted from an actual icing test on a 3-ft chord NACA 23012 airfoil model. The ice was simulated using various sizes of grit roughness and geometrically scaled to the 1.5-ft chord models used for these tests. Performance data were acquired for each of the airfoils with these ice simulations over a large angle-of-attack range at a Reynolds number of 1.8×10^6 and a Mach number of 0.18. Uniform roughness in the form of 80- and 150-grit sandpaper was also applied to the airfoil leading edge and tested.

The results for the ice simulations tested on the NACA 23012 airfoil were validated against previous tests of a 3-ft chord model that used castings of the actual ice shapes. Agreement between these tests was excellent and proved (at least for this case) that the ice could be successfully scaled down by the ratio of the chord lengths and simulated with relatively simple methods. As shown in previous studies, the performance degradation resulting from the intercycle ice simulations was severe. For the NACA 23012 airfoil, the maximum lift coefficients were reduced to a range of 0.65 to 0.80 from a clean value of 1.47. Performance effects, in terms of maximum lift coefficient, were less severe for the other two airfoils. The NLF 0414 airfoil maximum lift coefficient was reduced to a range of 0.90 to 1.05 from a clean value of 1.34 with the intercycle ice simulations. These same simulations reduced the maximum lift coefficient of the NACA 3415 airfoil to a range of 0.85 to 0.95 from a clean value of 1.37.

The reductions in maximum lift were most severe for the NACA 23012 airfoil, followed by the NACA 3415 and NLF 0414 airfoils. The NACA 23012 airfoil generated most of its lift from large suction pressures near the leading edge. The presence of the simulated ice prevented the formation of these large suction pressures, and hence the lift was substantially reduced. In the case of the other two airfoils, the pressure loading was distributed more uniformly along the chord, and resulting maximum lift penalties were smaller. The lift penalties at low-to-moderate lift coefficients for the NLF 0414 and the NACA 3415 airfoils were more severe than for the NACA 23012. The former two airfoils' moderate pressure loading was more adversely affected at lower lift coefficients by the presence of the ice than for the front-loaded NACA 23012 airfoil.

Tests conducted with the uniform roughness on the NACA 23012 airfoil were also validated against previous 36-in. chord model data. These results also showed that these roughness heights could simply

be scaled by the ratio of the chord lengths. The performance degradation resulting from the standard roughness was substantially less than that caused by the intercycle ice simulations. These effects, in terms of maximum lift, were more severe for the NACA 23012 and NACA 3415 airfoils, while the NLF 0414 was least affected.

Acknowledgments

References

[1]Shin, J., and Bond, T. H., "Surface Roughness Due to Residual Ice in the Use of Low Power Deicing Systems," NASA TM-105971, Jan. 1993; also AIAA Paper 93-0031, Jan. 1993.

[2]Albright, A. E., Kohlman, D. L., Schweikhard, W. G., and Evanich, P., "Evaluation of a Pneumatic Boot Deicing System on a General Aviation Wing Model," NASA TM-82363, June 1981.

[3]Bowden, D. T., "Effect of Pneumatic De-Icers and Ice Formations on Aerodynamic Characteristics of an Airfoil," NACA TN-3564, Feb. 1956.

[4]Jackson, D. G., and Bragg, M. B., "Aerodynamic Performance of an NLF Airfoil with Simulated Ice," AIAA Paper 99-0373, Jan. 1999.

[5]Gile-Laflin, B. E., and Papadakis, M., "Experimental Investigation of Simulated Ice Accretions on a Natural Laminar Flow Airfoil," AIAA Paper 2001-0088, Jan. 2001.

[6]Broeren, A. P., Addy, H. E., Jr., and Bragg, M. B., "Effect of Intercycle Ice Accretions on Airfoil Performance," AIAA Paper 2002-0240, Jan. 2002.

[7]Broeren, A. P., Bragg, M. B., and Addy, H. E., Jr., "Effect of Intercycle Ice Accretions on Airfoil Performance," *Journal of Aircraft*, Vol. 41, No. 1, 2004, pp. 165–174.

[8]Lee, S., "Effect of Supercooled Large Droplet Icing on Airfoil Aerodynamics," Ph.D. Dissertation, Dept. of Aeronautical and Astronautical Engineering, Univ. of Illinois, Urbana, IL, May 2001.

[9]Lee, S., and Bragg, M. B., "Investigation of Factors Affecting Iced-Airfoil Aerodynamics," *Journal of Aircraft*, Vol. 40, No. 3, 2003, pp. 499–508.

[10]Lee, S., and Bragg, M. B., "Effect of Simulated-Spanwise Ice Shapes on Airfoils: Experimental Investigation," AIAA Paper 99-0092, Jan. 1999.

[11]Lee, S., and Bragg, M. B., "Experimental Investigation of Simulated Large-Droplet Ice Shapes on Airfoil Aerodynamics," *Journal of Aircraft*, Vol. 36, No. 5, 1999, pp. 844–850.

[12]Rae, W. H., and Pope, A., *Low-Speed Wind Tunnel Testing*, Wiley, New York, 1984, pp. 349–362, 449.

[13]Kline, S. J., and McClintock, F. A., "Describing Uncertainties in Single-Sample Experiments," *Mechanical Engineering*, Vol. 75, Jan. 1953, pp. 3–8.

[14]Coleman, H. W., and Steele, W. G., *Experimentation and Uncertainty Analysis for Engineers*, Wiley, New York, 1989, pp. 40–118.

[15]Broeren, A. P., and Bragg, M. B., "Effect of Residual and Intercycle Ice Accretions on Airfoil Performance," Rep. DOT/FAA/AR-02/68, May 2002.

[16]Addy, H. E., Jr., and Chung, J. J., "A Wind Tunnel Study of Icing Effects on a Natural Laminar Flow Airfoil," AIAA Paper 2000-0095, Jan. 2000.

[17]Morgan, H. L., Ferris, J. C., and McGhee, R. J., "A Study of High-Lift Airfoils in the Langley Low-Turbulence Pressure Tunnel," NASA TM 89125, July 1987.

[18]Abbott, I. H., and von Doenhoff, A. E., *Theory of Wing Sections*, Dover New York, 1959, pp. 124–128, 480, 490.